Available online at www.sciencedirect.com

ScienceDirect

Ceramics International 40 (2014) 367–374

CERAMICS INTERNATIONAL

www.elsevier.com/locate/ceramint

Novel reduced toxic route synthesis and characterization of chemical bath deposited ZnSe thin films

G.L. Agawane[a], Seung Wook Shin[b,d], M.P. Suryawanshi[a], K.V. Gurav[a], A.V. Moholkar[a], Jeong Yong Lee[b,d], P.S. Patil[a], Jae Ho Yun[c,*], Jin Hyeok Kim[a,**]

[a]Department of Materials Science and Engineering, Chonnam National University, Gwangju 500-757, South Korea
[b]Department of Materials Science and Engineering, KAIST, Daejeon 305-701, South Korea
[c]Photovoltaic Research Group, KIER, Jang-Dong, Yuseong-Gu, Daejeon 305-343, South Korea
[d]Center for Nanomaterials and Chemical Reactions, Institute for Basic Science, Daejeon 305-701, South Korea

Received 22 April 2013; received in revised form 6 May 2013; accepted 4 June 2013
Available online 17 June 2013

Abstract

The synthesis of chemical bath deposited zinc selenide (ZnSe) thin films using a mixture of non-toxic complexing agent tri-sodium citrate (Na_3-citrate) and hydrazine hydrate (HH) and their physico-chemical properties are reported. Various amounts of complexing agent Na_3-citrate and HH solutions were prepared and used, listed as A, B, C, D, E and F. The effects of Na_3-citrate and HH concentration on the morphological, structural, compositional, chemical and optical properties of ZnSe thin films were investigated by field emission scanning electron microscopy (FE-SEM), atomic force microscopy (AFM), X-ray diffraction (XRD), X-ray photoelectron spectroscopy, Energy dispersive X-ray spectroscopy (EDS) and ultraviolet–visible spectroscopy, respectively. FE-SEM and AFM studies revealed that the uniformity of the ZnSe thin films decreased whilst RMS values increased for the films deposited from solutions A to F. XRD studies showed that the ZnSe thin films had no well resolved peaks showing an amorphous nature while peaks from (111), (220) and (311) planes corresponding to the ZnSe cubic phase were observed for the film deposited with solution A. EDS analysis revealed that the presence of Zn atom in the ZnSe thin films increased for the films deposited from solutions A to F. UV–visible study showed that the band gap energy increased from 2.65 to 3.55 eV for the ZnSe thin films deposited from solutions A to F.

Keywords: Chemical bath deposition; Non-toxic complexing agent; Buffer layers; Growth mechanism; Cu(In,Ga)Se_2 Solar cell

1. Introduction

Recently, Cu(In,Ga)Se2 (CIGS)-based thin film solar cells (TFSCs) have achieved the highest power conversion efficiency (PCE) of 20.3% [1]. The CIGS TFSCs are typically fabricated using chemical bath deposited CdS (CBD-CdS) thin films as a buffer layer. The buffer layer plays a vital role in the TFSCs, where it is employed between an absorber layer and a transparent conducting oxide layer, since it adjusts the appropriate interface charge and reduces chemical modification and lattice mismatch between the two layers, which results from chemical species in the sensitive surface of the absorber layer and junction regions [2,3]. Although the CBD-CdS buffer layer provides the above mentioned advantages for outstanding TFSCs performance, light with wavelength lower than 520 nm cannot be transmitted through the absorber layer due to the relatively narrow band gap energy of 2.4 eV. [4,5]. This results in a drop of the quantum efficiency in comparison to the theoretical efficiency [5]. In addition, the CBD-CdS in CIGS-based TFSCs creates a large amount of Cd containing waste during the deposition process [6]. Several major Cd poisoning incidents occurred in the early to mid-20th century all over the world [7,8]. Therefore, the Cd based buffer layer should be replaced for two reasons; (i) further improvement in the short circuit current (I_{sc}), which can be achieved using a wide band gap material and (ii)

*Corresponding author. Tel.: +82 42 860 3199; fax: +82 42 860 3539.
**Corresponding author. Tel.: +82 62 530 1709; fax: +82 62 530 1699.
E-mail addresses: yunjh92@kier.re.kr (J.H. Yun), jinhyeok@chonnam.ac.kr (J.H. Kim).

0272-8842/$ - see front matter © 2013 Elsevier Ltd and Techna Group S.r.l. All rights reserved.
http://dx.doi.org/10.1016/j.ceramint.2013.06.011

environmentally friendly synthesis process. Among the various alternatives such as ZnO, ZnS, ZnSe, In_2S_3 and InSe [9–13], the wide band gap materials like zinc sulphide (ZnS) with a band gap energy of 3.7 eV and zinc selenide (ZnSe) with band gap energy of 2.7 eV are the best candidates since they are economically priced and create low conduction band offsets [3,6,14]. Additionally these materials are most appropriate for their use in photoluminescent, electroluminescent devices and in short wavelength emitting diodes due to their wide band gap energy [15–17].

Recently, CIGS-based TFSCs using CBD-ZnS and CBD-ZnSe buffer layers having efficiencies of 18.6% and 15.7% are reported, respectively [18,11]. Though the TFSCs using CBD-ZnS buffer layers have achieved higher PCE than ZnSe, CBD-ZnS in the CIGS-based TFSC result in the mismatched band alignment between individual layers [19]. This characteristic of CBD-ZnS buffer layers creates a high conduction band offset in the heterojunction, which acts as a barrier for the electron movement towards both the grids giving rise to lower PCE of CIGS based TFSCs than that using CBD-CdS [19]. The evaluation of the diverse properties of the ZnS buffer layer show that ZnSe is a promising candidate to solve the low PCE problem due to its relatively wide band gap energy and possibility of good band gap alignment matching as reported for the CIGS TFSC structure [11].

Generally, the CBD-ZnSe thin films are prepared from an aqueous solution of Zn salt and selenourea in a hot basic medium using complexing agents for the controlled growth of Zn^{2+} ion concentration [17,20]. The K_{sp} of ZnSe is very low (10^{-31}) [17] as compared to CdS (10^{-27}) [21] and ZnS ($10^{-24.7}$) [3], therefore, growing uniform ZnSe thin films is an art wherein the usual practices are of no use and one has to use an appropriate complexing agent. Many researchers therefore introduced hydrazine hydrate (HH), as a complexing agent, which controls Zn^{2+} ion concentration during the deposition process in order to obtain uniform ZnSe thin films [11,17,20]. Several researchers have reported that the addition of HH in a reaction bath improves adherence, uniformity, homogeneity, and growth rate of ZnSe thin films, and that HH plays the role of side complexing agent [11,17,20,22]. Although the previous reports have indicated uniform, adhered ZnSe thin films with improved growth rate using HH, the highly flammable, toxic and carcinogenic nature of HH cannot be ignored in concern with human beings and environmental safety [3].

Our earlier reports showed that the CBD-ZnS thin films can be formed easily using Na_3-citrate. The Na_3-citrate forms strong citrate anions ($(C_6H_5O_7)^{3-}$) in the basic bath [3,6], and the use of various molar concentrations of Na_3-citrate cause the growth of thin films by different mechanisms [6]. In addition, the various physico-chemical properties like transmittance, thin film thickness, uniformity and the growth rate of the thin films are found to be principally dependent on the concentration of Na_3-citrate [6,23,24]. Various metal ions like Zn^{2+}, Fe^{3+}, Ca^{2+}, Ag^{+}, and Mg^{2+} can be complexed and their growth controlled in CBD by the use of three carboxylate groups [25]. The outstanding complexing characteristics of Na_3-citrate such as its strong complexing nature, nontoxicity, and low cost encouraged us to deposit the ZnSe thin films using it and complexing it with HH. Additionally, the use of a mixture of complexing agents gives rise to high quality CBD Zn-compound thin films, which are more eco-friendly and have a better deposition rate as confirmed by our previous report [26]. Therefore, the synthesis of ZnSe thin films with a mixture of Na_3-citrate and HH has been carried out.

As per our knowledge, in this work we report for the first time the CBD-ZnSe thin films deposited by the use of Na_3-citrate with HH at 80 °C. The effects of different amounts of Na_3-citrate and HH on the morphological, structural, chemical, compositional and optical properties of CBD-ZnSe thin films were investigated.

2. Experimental details

Chemicals used for the deposition were of analytical grade and were purchased from Sigma-Aldrich. They include zinc sulphate ($ZnSO_4$), selenourea ($SeC(NH_2)_2$), ammonia (25%) and the complexing agent hydrazine hydrate (HH) along with non-toxic complexing agent tri-sodium citrate (Na_3-citrate). The solutions were prepared in deionized water and films were deposited on $26 \times 76 \times 2$ mm^3 glass substrates. The reaction bath was prepared using 10 mL 0.5 M $ZnSO_4$ and 10 mL 0.4 M ($SeC(NH_2)_2$). Different quantities of the 0.5 M non-toxic complexing agent Na_3-citrate were used along with 27% HH. The total quantity of the complexing agent solution was made to 10 mL. Table 1 shows the ZnSe thin films deposited by the use of six different mixtures of Na_3-citrate and HH as complexing agents. The prepared solutions with various Na_3-citrate and HH quantities are shown in Table 1 and are entitled A, B, C, D, E and F. The pH was adjusted to 10 by adding 25% ammonia (NH_4OH) solution. Finally, a sufficient amount of deionized water was added to make the total volume of the deposition bath 100 mL. Prior to deposition, the glass substrates were ultrasonically cleaned with acetone followed by rinsing in methanol, isopropyl alcohol and deionized water for 10 min, respectively. The glass substrates were mounted vertically on a specially designed substrate holder. The temperature of the reaction bath was maintained at 80 °C. After deposition for 2 h, the glass substrates were removed, washed several times with deionized water and dried naturally. Vigorous oxidation of the surface selenium of the film occurs when it is exposed to air, therefore, the thin films were kept in a glove-box in an Ar atmosphere. The resultant films were

Table 1
List of the solutions prepared as a complexing agent.

Solution	Na_3-citrate (mL)	Hydrazine hydrate (mL)	Total volume (mL)
A	0	10	10
B	2	8	10
C	3	7	10
D	5	5	10
E	7	3	10
F	8	2	10

homogenous, whitish in colour and adhered well to the glass substrate.

The cross-sectional and morphological study of the deposited thin films were observed by field emission scanning electron microscopy (FE-SEM, Model: JSM-6701F, Japan) and atomic force microscopy (AFM, Digital Instrument, Nanoscope III, USA) operated at room temperature. The structural properties of the thin films were observed by high-resolution X ray diffraction spectroscopy (XRD, X'pert PRO, Philips, Eindhoven, The Netherlands) operated using a grazing incidence diffraction mode. The chemical binding energy investigations of the ZnSe thin films were carried out by X-ray photoelectron spectroscopy (XPS, VG Multilab 2000, Thermo Scientific, UK). The binding energies in the spectrometer were calibrated using a carbon 1s line at 285.0 eV. The chemical compositions were examined using an energy dispersive spectrometer (EDS) system attached to the FE-SEM (JEOL, JSM-7500F, Japan). The optical properties of the thin films were observed using UV–visible spectroscopy (Cary 100, Varian, Mulgrave, Australia).

3. Results and discussion

Fig. 1 shows surface and cross-sectional FE-SEM images of the ZnSe thin films deposited with different solutions viz., A ((a) and (b)), B ((c) and (d)), C ((e) and (f)), D ((g) and (h)), E ((i) and (j)) and F ((k) and (l)). FE-SEM results for the solution A deposited ZnSe thin film (Fig. 1(a) and (b)) show a uniform nature and the thin film consists of round shaped grains with an average grain size of nearly 200 nm. The thickness of the solution A deposited ZnSe thin film is 180 nm. The ZnSe thin film deposited with solution B (Fig. 1(c) and (d)) shows somewhat decreased uniformity, reduced grain size of 170 nm and reduction in the thickness to 120 nm. The ZnSe thin film deposited using solution C (Fig. 1(e) and (f)) shows an increased grain size and increased voids as compared to the earlier films and the thickness increased up to 195 nm. The ZnSe grain size further decreased for the films deposited with increased amount of tri-sodium citrate (Na_3-citrate) and decreased amount of HH i.e. from the solution D to F (Fig. 1(g)–(l)). The thicknesses of all the ZnSe thin films are irrespective of the use of solutions due to discontinuity in the surface characteristics. Although most of the above discussed films show non-uniformity, the FE-SEM results obtained for the ZnSe thin film are significantly better than those reported elsewhere [20,27].

Microscopic information and surface roughness studies were carried out by the AFM technique. Fig. 2(a)–(f) shows $1 \times 1\ \mu m^2$ size 3D images the ZnSe thin films deposited using various solutions from A to F and Fig. 2(g) shows a graph of RMS values of the ZnSe thin films against various solutions. The AFM study for the solution A deposited thin film indicates that the RMS value of the film is very low, ~25 nm and the thin film shows a smooth surface with some voids. The RMS value of solutions

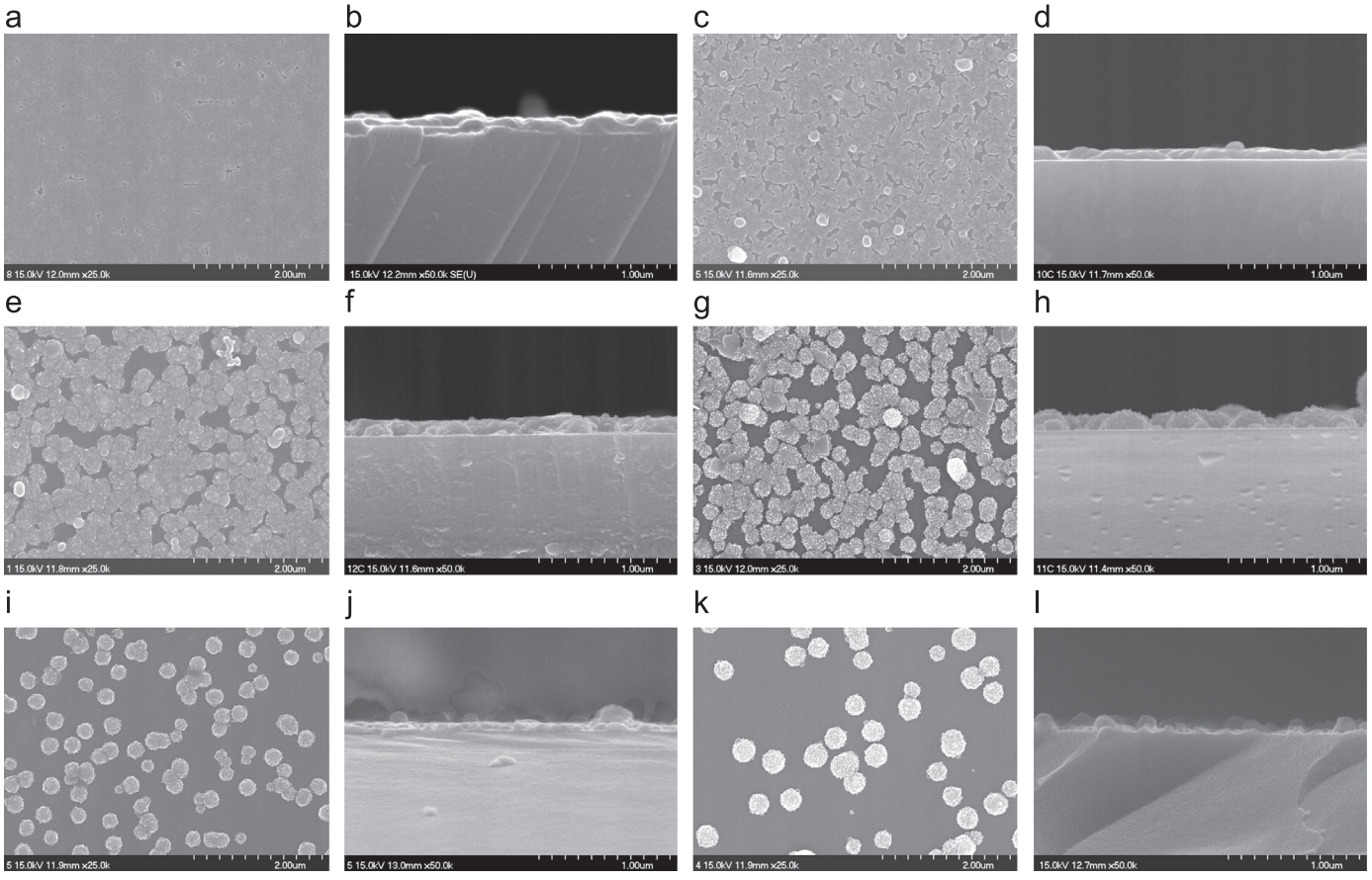

Fig. 1. Surface and cross-sectional FE-SEM images of the ZnSe thin films deposited using various solutions viz., A (a, b), B (c, d), C (e, f), D (g, h), E (i, j), and F (k, l).

B–F deposited ZnSe thin films steadily goes on increasing from 30 to 64 nm. In addition, the grain size of the ZnSe thin films decreased when Na_3-citrate concentration is increased. A few areas for solutions E and F deposited thin film show a very uniform surface morphology without any voids.

Noticeable information about the thin film growth mechanism is obtained from the above mentioned FE-SEM and AFM results, and a similar type of the growth mechanism has been described by our previous report [6]. The thin films with a dense and continuous microstructure can be deposited by the use of solution A. However, many voids and discontinuous microstructures are observed for the thin films deposited with solution B–E. In addition, the thickness of the deposited thin films decreases dramatically with increasing Na_3-citrate's concentration. These different characteristics of the thin films are attributed to the different concentrations of Zn–

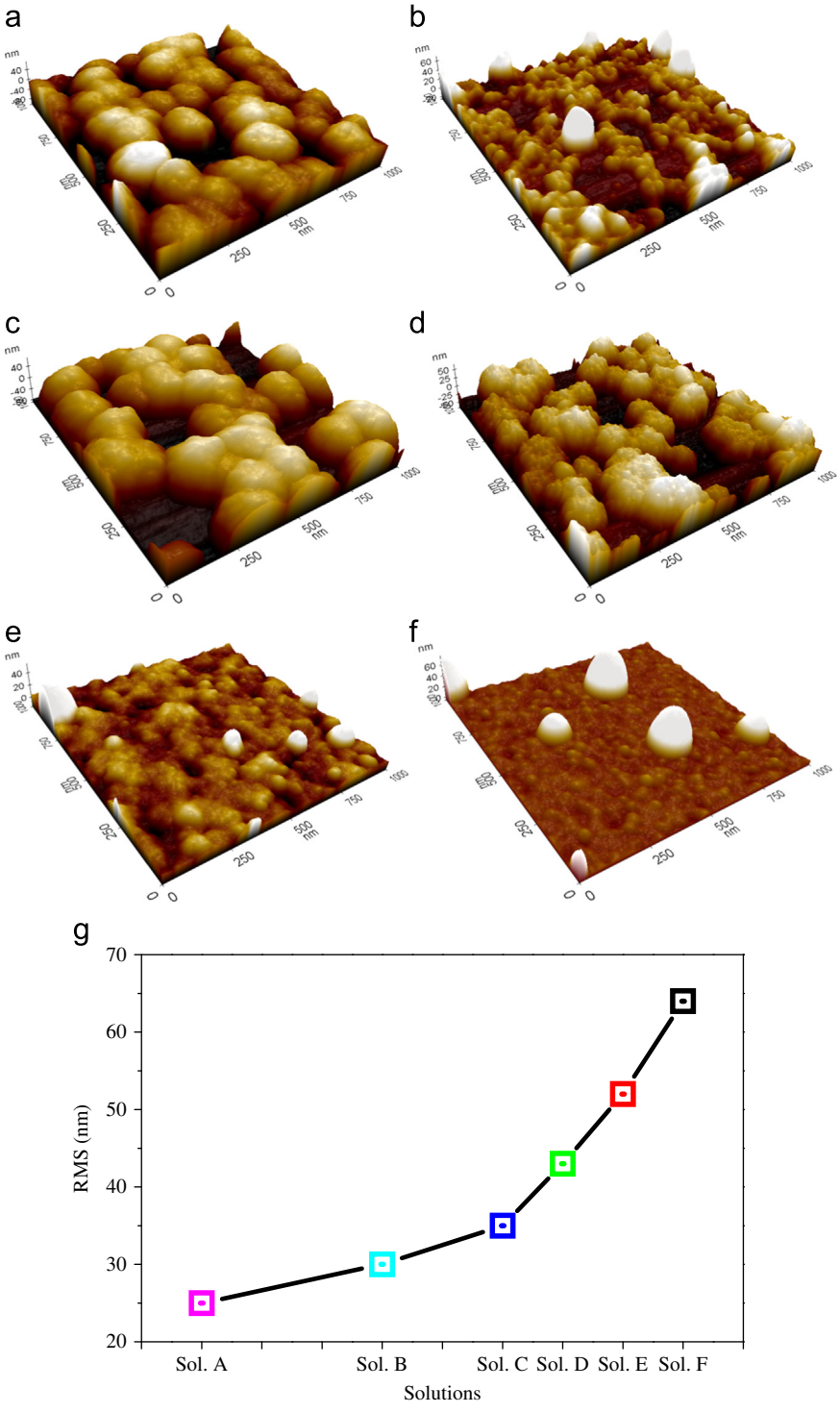

Fig. 2. 3D AFM images of the ZnSe thin films deposited using various solutions viz., A (a), B (b), C (c), D (d), E (e), and F (f) while graph (g) shows RMS values vs. use of different solutions.

[complexing agent]$^{2+}$ in different solutions. Generally, the growth mechanism of the ZnSe thin film is described as the Zn–[complexing agent]$^{2+}$ ions react with Se^{2-} ions in the solution or substrate surface [17,21]. Therefore, a suitable complexing agent plays a very important role for the stable ZnSe thin films deposition since the complexing agent reduces the Zn ion releasing rate in the reaction bath [17,21].

In the case of the reaction solution without Na_3-citrate (solution A), the NH_3 and HH are present and act as complexing agents. The NH_3 and HH react with Zn^{2+} ions, which produce $[Zn(NH_3)_n]^{2+}$ and $[Zn(HH)_n]^{2+}$ ions in the reaction bath. From earlier studies, it has become known that HH is a very strong complexing agent, indicating that the Zn^{2+} ions can fully react with the complexing agent [17,20,22]. At a higher temperature, the Zn^{2+} ions are released from the [Zn–complexing agent]$^{2+}$ and free Zn^{2+} ions directly react with Se^{2-} ions. This behaviour results in the generation of many heterogeneous nucleation sites allowing thin films to easily form with a uniform and dense microstructure [17]. In contrast, the reaction solutions B–D consist of a low HH concentration, therefore, many Zn–[complexing agent]$^{2+}$ ions such as $[Zn(NH_3)_n]^{2+}$, $[Zn(HH)_n]^{2+}$ and $[Zn(Na_3\text{-citrate})_n]^{2+}$ ions as well as a small amount of free Zn^{2+} ions are present in these solutions as compared to solution A. Zn–[complexing agent]$^{2+}$ ions easily react with Se^{2-} ions, which leads to the large grains and free Zn^{2+} ions also react with OH^- and O^{2-} ions [6]. These chemical behaviours lead to more homogeneous nucleation and less heterogeneous nucleation. Finally, the deposited thin films consisted of large grains with thin thicknesses. In the case of high concentration of Na_3-citrate and low concentration of HH (solution E and F) solutions, there are higher numbers of free Zn^{2+} ions in the reaction bath as compared to those of solutions A, B, C and D, these characteristics result in a lower number of grains, non-uniformity and thin thickness [6].

Fig. 3 shows XRD patterns of the ZnSe thin films deposited with different solution concentration. The XRD pattern for the ZnSe thin film deposited with solution A shows three broad peaks at 27.5°, 47.4° and 54.5° corresponding to the (111), (220) and (311) planes from the ZnSe cubic phase respectively [JCPDS data file No.: 80-0021]. This crystal behaviour confirms the polycrystalline nature of the ZnSe thin film and significantly similar results are reported elsewhere [15,20]. No secondary phases such as ZnO and $Zn(OH)_2$ are observed for the ZnSe thin film deposited with Solution A. In the case of the ZnSe thin film deposited using solution B, the peak intensity for the (111) plane for the cubic phase dramatically decreased and no peaks for the (220) and (311) planes are observed. On the other hand, no peaks are observed for the ZnSe thin films deposited using solutions C, D, E and F indicating an amorphous nature. The poorer crystallinity of the ZnSe thin films is attributed to the different growth mechanisms with different reaction solutions as discussed above [6].

The chalcogenide based materials synthesised by chemical bath deposition in basic mediums suffer from the presence of the metal–OH compounds and these metal–OH compounds are grounds of the different characteristics such as poor crystallinity, low growth rate and meta stable band gap energy [6,28–29].

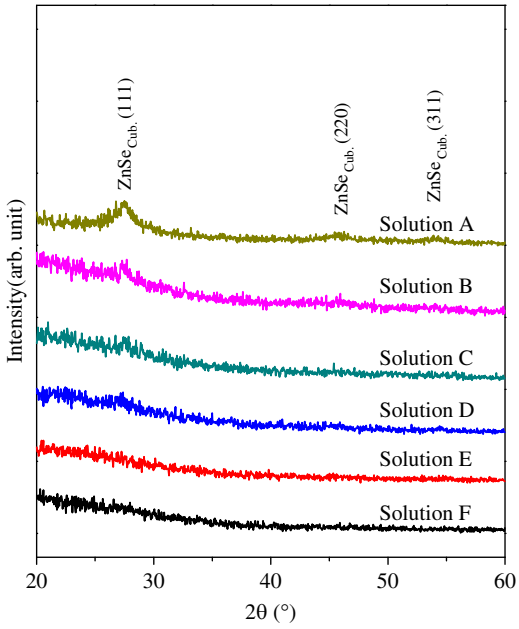

Fig. 3. XRD patterns of the ZnSe thin films deposited using different solutions.

Therefore, in order to reveal the state of the constituent elements, as well as Zn–Se and Zn–OH binding energies in the CBD-ZnSe thin films, XPS surveys are recorded. Fig. 4 shows XPS core level spectra of the Zn $2p^{3/2}$ (a) and Se 3d (b) of the ZnSe films deposited using various solutions. The binding energy of the Zn $2p^{3/2}$ atomic state (Fig. 4(a)) is observed at 1022.0 eV resulting from the Zn–Se bonding for the films deposited with solutions A, B, C, and D. While, in the case of solutions E and F, the binding energy shifted slightly towards higher energy and observed at 1022.3 eV resulting from the Zn–OH bonding. This confirms that there are more Zn–OH bonds for the films deposited with solutions E and F than the films deposited with solutions A, B, C and D. These results are significantly similar to those reported elsewhere [3,6,28]. This behaviour is well explained by the above mentioned growth mechanism, which shows the films deposited with solutions E and F as having the most voids and excess non-uniform nature. The reasons for the high number of Zn–OH bonds for the films deposited with solutions E and F can be attributed to the higher amount of citrate ions having a lower ability to hold the Zn^{2+} ions due to a weaker complexing nature than the HH [17], which cannot control the growth of Zn–OH bonds due to the greater affinity of Zn towards OH^- ions than Se^{2-} ions. While in the case of the higher amount of HH, i. e. the films deposited with the solutions A, B, C and D, the growth mechanism acts in the reverse manner, since the HH has a stronger complexing nature than the Na_3-citrate, which gives rise to higher number Zn–Se bonds than Zn–OH bonds. The binding energies of Se $3d^{5/2}$ and Se $3d^{3/2}$ (Fig. 4(b)) are observed at 54.7 and 55.5 eV, respectively, resulting from the Zn–Se bonding for all the ZnSe thin films. The explanation of Se 3d atomic state from the Zn–Se bonds is much similar to that reported elsewhere [28]. Reports have shown that CBD-ZnSe thin films gives rise to Se metal (Se°) due to the surface oxidation [28], but the XPS results obtained in our study do not show the presence of Se°

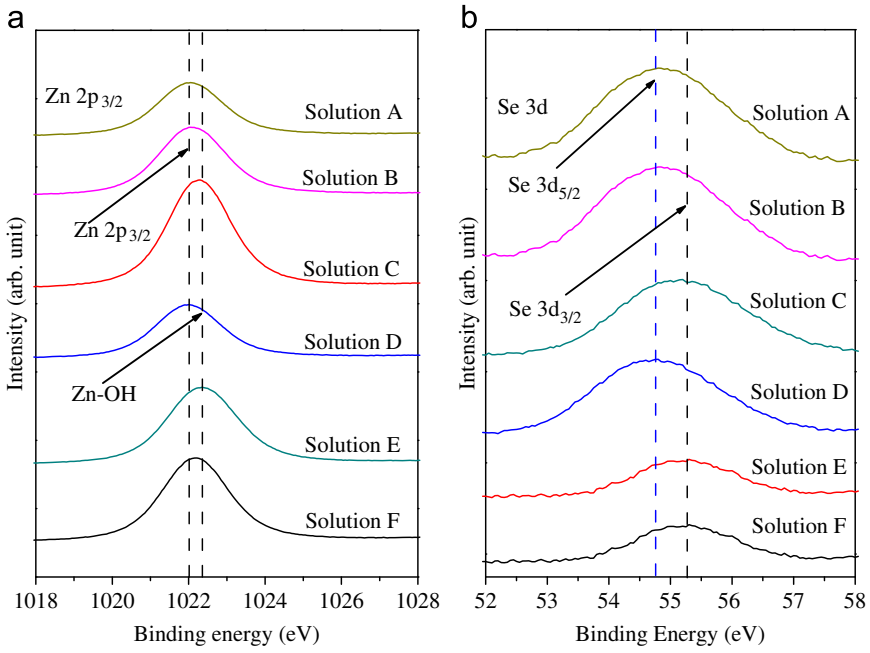

Fig. 4. Core level XPS spectra of Zn $2p_{3/2}$ (a) and Se 3d (b) of the ZnSe thin films deposited using various solutions.

bonding. The signal intensity is irrespective of the type of solution used. Zn–O bonds might be formed during the deposition of ZnSe, but its formation during CBD is not very likely to be in high concentrations, so it is believed that it may convert into $Zn–(OH)_x$ [28]. In addition, for Zn and Se spectra no shoulders on the lower or higher energy side are observed, which indicates pure Zn–Se formation along with fairly low Zn–OH bonding.

Table 2 shows the elemental analysis studied by the EDS technique of CBD-ZnSe thin films deposited using different solutions. It can be seen that the atomic percentage of Zn and Se in the ZnSe films deposited with solution A is 51.0 and 49.0%, respectively and the film shows good stoichiometry. Reasons for this stoichiometric Zn:Se ratio can be attributed to the presence of an appropriate amount of complexing agent HH, which does not allow the formation of Zn–OH bonds from unwanted Zn^{2+} ions. Further, for the ZnSe thin films deposited using solutions B–F, the Se at% decreases from 45.5 to 39.9 at% along with steady increase in the Zn at% from 54.5 to 60.1 at%. This increase in Zn content and decrease in Se content may be attributed to the uncontrolled growth of Zn^{2+} ions due to excess amount of citrate ions and less amount of HH ions, which cannot hold Zn^{2+} ions strongly. The EDS results obtained for the ZnSe thin films are in agreement with XRD (Fig. 3) and XPS (Fig. 4(a) and (b)) results, which show that except for the films deposited with solutions A and B, all the films show amorphous nature and the films deposited with solutions E and F show Zn–Se bonds along with Zn–OH bonds, respectively. Although the films deposited using solutions B–F deviate slightly from the stoichiometry, the obtained elemental analysis results are satisfactory compared to the films deposited by only use of HH as a complexing agent in the literature [28].

Optical characteristics like transmittance, absorbance and refractive index of the buffer layers are the outcomes of

Table 2
Elemental analysis of the ZnSe thin films deposited using various solutions.

Element	Solution					
	A	B	C	D	E	F
Zn (at%)	51.0	54.5	55.2	58.04	58.95	60.1
Se (at%)	49.0	45.5	44.8	41.96	41.05	39.9

thickness, uniformity and RMS value [3,23,30]. The films with minimum thickness, uniform nature (this forms less scattering centres) and least RMS values show high transmission with a sharp absorption edge [6]. In addition, the crystalline nature of the film is responsible also for determining the band gap energy of the film [30,31].

Therefore, to study the ZnSe thin films optical properties with UV–Visible light, the films were analysed in the 200–800 nm wavelength range. Fig. 5(a) shows percentage of transmission and Fig. 5(b) shows the plot of $(\alpha h\upsilon)^2$ vs. photon energy ($h\upsilon$) in eV obtained by extrapolating the straight-line portion of the curves at $\alpha = 0$. From Fig. 5(a) it can be seen that all the films show 55–88% of transmittance in the visible range. The transmittance of the ZnSe thin films increased continuously from solution A to solution F. The films have shown varied absorption edges in the near ultraviolet wavelength region from 370 to 270 nm.

The reasons for higher wavelength absorption edges are as follows: pure ZnSe is formed when the films are deposited with solutions A and B, since sufficient amounts of HH and Na_3-citrate are present, which allows deposition of uniform ZnSe thin films without growing secondary phases, hence the film shows a steep absorption edge at 370 nm [17]. While, reasons the lower absorption edges in case of the ZnSe films deposited with

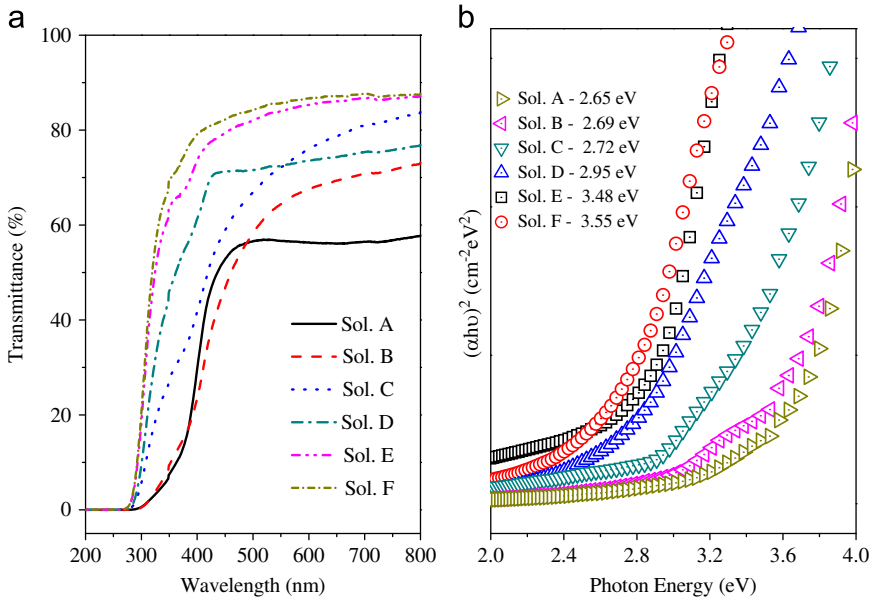

Fig. 5. UV–visible transmittance spectra from 200 to 800 nm (a) and the plot of $(\alpha h\upsilon)^2$ vs. photon energy (b) of the ZnSe thin films deposited using various solutions.

solutions C, D, E and F which gives rise to the formation of ZnSe film with insignificant ZnO or Zn–OH compound formation due to an inadequate amount of the strong complexing agent. Since the K_{sp} of ZnSe is very low [17], it needs a very sturdy complexing agent with its proper amount, therefore, these films have shown absorption edges in the range of 330–270 nm. Fig. 5(b) shows the band gap energies of the CBD-ZnSe thin films. The ZnSe films have shown varied band gap energies from 2.65 to 3.55 eV. The films deposited with solutions A and B show the formation of pure ZnSe, which has the band gap energy of 2.65 and 2.69 eV. The insignificantly lower band gap energy of the ZnSe thin films than the bulk ZnSe (2.7 eV) [17], indicates the formation of ZnSe cubic phase [32]. In addition, the band gap energies of the ZnSe thin films deposited with solutions A and B are in good agreement with our XRD, XPS and FE-SEM results. While for the films deposited with solutions C and D, the band gap energies vary significantly. The films deposited with solutions C and D show relatively wide band gap energies of 2.72 and 2.95 eV, respectively. The wide band gaps of the films are attributed to the presence of more scattering centres, non-uniform nature and insignificant oxide phases originated from excess Zn^{2+} ions growth [28]. The films deposited with solutions E and F show wide band gap energies of 3.48 and 3.55 eV, respectively and the reasons for this wide band gap energy are attributed to increased non-uniformity and excess hydroxide phases present in the films.

4. Conclusions

This study shows a simple way to deposit the ZnSe thin films in aqueous zinc sulphate and selenourea bath using the non-toxic complexing agent Na_3-citrtate along with decreased amounts of HH. FE-SEM studies showed that the uniformity was decreased for the ZnSe thin films deposited from solutions A to F. Therefore, the surface morphology was found to be strongly dependent on the amount of Na_3-citrate and HH. The highest RMS value was observed for the film deposited with solution F and lowest RMS value for film deposited with solution A. Structural characterizations showed that the ZnSe films were in amorphous nature, except for the films deposited with solutions A and B which showed ZnSe cubic phase formation. The XPS technique for the ZnSe thin films showed that the Zn–Se bonding were present with slight Zn–OH bonding. Optical studies showed that the films were highly transparent and the entire films exhibited good adherence to the glass substrate.

The direct band gap energies of the ZnSe thin films varied from 2.65 to 3.55 eV, depending upon the solution used. Although, our first report for the deposition of chemical bath ZnSe by a less toxic route shows wide or narrow band gaps, an amorphous ZnSe phase, less uniformity and relatively higher oxygen contents for the films deposited with solutions C–F, all the results are satisfactory. Therefore, this study has motivated us to engineer the band gaps of ZnSe with a uniform deposition by the use of a non-toxic complexing agent Na_3-citrate. Thus, the studies for optimizing the various parameters are underway.

Acknowledgements

This work was supported by the Human Resources Development program (No. 20124010203180) of the Korea Institute of Energy Technology Evaluation and Planning (KETEP) grant funded by the Korea government Ministry of Trade, Industry and Energy. Also, this work was partially supported by Centre for Inorganic Photovoltaic Materials (2012-0001170) grant funded by the Korea government (MEST).

References

[1] P. Jackson, D. Hariskos, E. Lotter, S. Paetel, R. Wuerz, R. Menner, W. Wischmann, M. Powalla, Progress in Photovoltaics: Research and Applications 19 (2011) 894.

[2] W. Wang, S.Y. Han, S.J. Sung, D.H. Kim, C.H. Chang, Physical Chemistry Chemical Physics 14 (2012) 11154–11159.

[3] S.W. Shin, S.R. Kang, J.H. Yun, A.V. Moholkar, J.H. Moon, J.Y. Lee, J.H. Kim, Solar Energy Materials and Solar Cells 95 (2011) 856–863.

[4] N.S. Das, P.K. Ghosh, M.K. Mitra, K.K. Chattopadhyay, Physica E 42 (2010) 2097–2102.

[5] M.M. Islam, S. Ishizuka, A. Yamada, K. Sakurai, S. Niki, K. Sakurai, K. Akimoto, Solar Energy Materials and Solar Cells 93 (2009) 970–972.

[6] G.L. Agawane, S.W. Shin, A.V. Moholkar, K.V. Gurav, J.H. Yun, J.Y. Lee, J.H. Kim, Journal of Alloys and Compounds 535 (2012) 53–61.

[7] B.T. Emmerson, Annals of Internal Medicine 73 (1970) 854–855.

[8] M. Kasuya, Water Science and Technology 42 (2000) 147–155.

[9] S.A. Vanalakar, S.S. Mali, R.C. Pawar, D.S. Dalavi, A.V. Mohalkar, H.P. Deshamukh, P.S. Patil, Ceramics International 38 (2012) 6461–6467.

[10] S. Xue, Ceramics International, 2013, in press.

[11] A. Ennaoui, S. Siebentritt, M. Ch., W. Lux-Steiner, F. Riedl, Karg, Solar Energy Materials and Solar Cells 67 (2001) 31–40.

[12] B. Yahmadi, N. Kamoun, C. Guasch, R. Bennaceur, Materials Chemistry and Physics 127 (2011) 239–247.

[13] H.M. Pathan, S.S. Kulkarni, R.S. Mane, C.D. Lokhande, Materials Chemistry and Physics 93 (2005) 16–20.

[14] F. Engelhardt, L. Bornemann, M. Kontges, T.h. Meyer, J. Parisi, E. Pschorr-Schoberer, B. Hahn, W. Gebhardt, W. Riedl, U. Rau, Progress in Photovoltaics: Research and Applications 7 (1999) 423.

[15] H. Metin, S. Durmus, S. Erat, M. Ari, Applied Surface Science 257 (2011) 6474–6480.

[16] C. Mehta, G.S.S. Saini, J.M. Abbas, S.K. Tripathi, Applied Surface Science 256 (2009) 608–614.

[17] J.M. Dona, J. Herrero, Journal of the Electrochemical Society 141 (1994) 205–210.

[18] M.A. Contreras, T. Nakada, M. Hongo, A.O. Pudov, J.R. Sites, In: Proceedings of the 3rd World Conference on Photovoltaic Energy Conversion, Osaka, Japan, May 11–18, 2003, p. 570.

[19] T. Nakada, M. Hongo, E. Hayashi, Thin Solid Films 431–432 (2003) 242–248.

[20] L. Chen, D. Zhang, G. Zhai, J. Zhang, Materials Chemistry and Physics 120 (2010) 456–460.

[21] T. Sugimoto, S. Chen, A. Murumatsu, Colloids and Surfaces A: Physiochemical and Engineering Aspects 135 (1998) 207–226.

[22] Y. Zhang, C. Hu, B. Feng, X. Wang, B. Wan, Applied Surface Science 257 (2010) 10679–210685.

[23] A.V. Moholkar, G.L. Agawane, K.U. Sim, Y.B. Kwon, D.S. Choi, K.Y. Rajpure, J.H. Kim, Journal of Alloys and Compounds 506 (2010) 794–799.

[24] G.L. Agawane, S.W. Shin, M.S. Kim, M.P. Suryawanshi, K.V. Gurav, A.V. Moholkar, J.Y. Lee, J.H. Yun, P.S. Patil, J.H. Kim, Current Applied Physics 13 (2013) 850–856.

[25] S. Cho, J.W. Jang, S.H. Jung, B.R. Lee, E. Oh, K.H. Lee, Langmuir 25 (2009) 3825–3831.

[26] S.W. Shin, S.R. Kang, K.V. Gurav, J.H. Yun, J.H. Moon, J.Y. Lee, J.H. Kim, Solar Energy 85 (2011) 2903–2911.

[27] P.P. Hankare, P.A. Chate, S.D. Delekar, M.R. Asabe, I.S. Mulla, Journal of Physics and Chemistry of Solids 67 (2006) 2310–2315.

[28] A.M. Chaparro, C. Maffiotte, M.T. Gutierrez, J. Herrero, Thin Solid Films 358 (2000) 22–29.

[29] H.R. Moutinho, M.M. Al-Jassim, F.A. Abulfotuh, D.H. Levi, P.C. Dippo, R.G. Dhere, L.L. Kazmerski, 1997, in: Proceedings of the 26th IEEE Photovoltaic Specialist Conference, IEEE, California.

[30] A.V. Moholkar, G.L. Agawane, K.U. Sim, Y.B. Kwon, K.Y. Rajpure, J.H. Kim, Applied Surface Science 257 (2010) 93–101.

[31] A. Goudarzi, G.M. Aval, R. Sahraei, H. Ahmadpoor, Thin Solid Films 516 (2008) 4953–4957.

[32] S. Soundeswaran, O. Senthil Kumar, R. Dhanasekaran, P. Ramasamy, R. Kumaresen, M. Ichimura, Materials Chemistry and Physics 82 (2003) 268–272.